1230 *Inorg. Chem.* **2010**, *49*, 1230–1237
DOI: 10.1021/ic902197f

Inorganic Chemistry
Article

Toward Verdazyl Radical-Based Materials: Ab Initio Inspection of Potential Organic Candidates for Spin-Crossover Phenomenon

Jean-Baptiste Rota, Boris Le Guennic, and Vincent Robert*

Université de Lyon, Laboratoire de Chimie, Ecole Normale Supérieure de Lyon, CNRS, 46 allée d'Italie, F-69364 Lyon, France

Received November 6, 2009

The origin of magnetic interactions in verdazyl-based radical stackings is examined using ab initio wave function and density functional theory (DFT) calculations. Starting from the reported crystal structure of the 1,1′-bis-(verdazyl)ferrocene diradical compound, the singlet−triplet energy difference has been evaluated on the basis of multireference difference dedicated configurations interaction calculations and suggested the innocent role of the ferrocene spacer. Using the underlying π-dimer verdazyl structures, the J variations and potential energy surfaces of parallel and antiparallel face-to-face arrangements have been studied with respect to the verdazyl−verdazyl separation to evaluate the Coulomb repulsion U and bandwidth W. While coupled-cluster CCSD(T) calculations are suggestive of a weak bond formation in both dimer arrangements ($\sim$40 kJ mol^{-1}), the DFT approach fails to reproduce the bonding character. The intrinsically delocalized character of the magnetic orbitals favors an $S = 0$ ground state, but importantly, the $S = 1$ spin state is also bound. A typical 0.4 Å increase (i.e., 10%) of the verdazyl−verdazyl equilibrium distance accompanying a 16 kJ mol^{-1} adiabatic energy difference is calculated between the $S = 0$ and $S = 1$ states. In this distance separation regime, we finally suggest that either a relative 1.2 Å slippage or a $\sim$42° relative orientation of the verdazyl rings is likely to give rise to a high-spin $S = 1$ ground state. These features are symptomatic of a bistable system, and an interpretation of the exchange interaction in verdazyl π-dimer structures in terms of spin transition is proposed.

1. Introduction

Electronic properties of molecular-based systems have attracted much attention since spectacular manifestations including superconductivity,[1] the spin-crossover phenomenon,[2,3] and valence tautomerism[4] have been observed. Thus, the preparation, characterization, and manipulation of molecular crystals have become an ever increasing active field of research with technologically relevant applications. A prime requirement along the synthetic routes is the suppression of the charge disproportionation by growing intermolecular interactions. With this goal in mind, organic radicals have considerably extended the building blocks panel in the popular field of molecular-based materials.[5−9] They can be used to design purely organic materials or metal-radical architectures.[10,11] In particular, the simultaneous presence of aromatic rings and nitrogen- or sulfur-rich moieties holding unpaired electrons is likely to bring the desired intermolecular interactions. Nevertheless, many organic radicals are known to be unstable since they exhibit a propensity to dimerization which suppresses the expected electro-active ligand character. Such dominant behavior among the organic radicals family is to be contrasted with experimental observations on verdazyl- or thiazyl-based radicals. Indeed, these organic species have recently received particular attention because of their stability and ligand and donor/acceptor

*To whom correspondence should be addressed. E-mail: vincent.robert@ens-lyon.fr.

(1) Yanase, Y.; Jujo, T.; Nomura, T.; Ikeda, H.; Hotta, T.; Yamada, K. *Phys. Rep.* **2003**, *387*, 1–149.
(2) Spin Crossover in Transition Metal Compounds I. In *Topics in Current Chemistry*; Gütlich, P., Goodwin, H. A., Eds.; Springer: New York, 2004; Vol. *233*.
(3) Spin Crossover in Transition Metal Compounds II. In *Topics in Current Chemistry*; Gütlich, P., Goodwin, H. A., Eds.; Springer: New York, 2004; Vol. *234*.
(4) Evangelio, E.; Ruiz-Molina, D. *Eur. J. Inorg. Chem.* **2005**, 2957–2971.
(5) Hicks, R. G.; Lemaire, M. T.; Thompson, L. K.; Barclay, T. M. *J. Am. Chem. Soc.* **2000**, *122*, 8077–8078.
(6) Preuss, K. E. *Dalton Trans.* **2007**, 2357–2369.
(7) Koivisto, B. D.; Hicks, R. G. *Coord. Chem. Rev.* **2005**, *249*, 2612–2630.
(8) Vostrikova, K. E. *Coord. Chem. Rev.* **2008**, *252*, 1409–1419.
(9) Train, C.; Norel, L.; Baumgarten, M. *Coord. Chem. Rev.* **2009**, *253*, 2342–2351.
(10) Rota, J.-B.; Norel, L.; Train, C.; Ben Amor, N.; Maynau, D.; Robert, V. *J. Am. Chem. Soc.* **2008**, *130*, 10380–10385.
(11) Norel, L.; Pointillart, F.; Train, C.; Chamoreau, L.-M.; Boubekeur, K.; Journaux, Y.; Brieger, A.; Brook, D. J. R. *Inorg. Chem.* **2008**, *47*, 2396–2403.
(12) Jornet, J.; Deumal, M.; Ribas-Arino, J.; Bearpark, M. J.; Robb, M. A.; Hicks, R. G.; Novoa, J. J. *Chem.—Eur. J.* **2006**, *12*, 3995–4005.
(13) Pointillart, F.; Train, C.; Herson, P.; Marrot, J.; Verdaguer, M. *New J. Chem.* **2007**, *31*, 1001–1006.

 Published on Web 01/05/2010

characteristics, not to mention their ability to grow three-dimensional organic networks.[5,6,10−16] In this respect, these organic radicals look like very promising candidates for the design of conducting and magnetic materials. The use of neutral radicals was considered since the presence of unpaired electrons within the constitutive units offers multifunctionality,[17] with several examples recently reported in the literature.[18−24] The simultaneous reduction of the Coulomb repulsion (U) and enlargement of the bandwidth (W) has been suggested to elaborate a metallic ground state. As featured examples, heterocyclic dithiazolyl radicals have been developed toward this end,[25] and the replacement of sulfur by selenium[26] has led to improved conductivities. Quite remarkably, a bistability regime was observed in structure involving π-stacking dimers.[24,25] A neutral thiazyl radical material exhibits room-temperature hysteresis loops as wide as 100 K.[24] Therefore, one may expect the making and breaking of weak bonds between the radicals to be of particular importance, and this should require particular attention. Recently, the magnetic measurements performed upon the 1,1′-bis(verdazyl)ferrocene diradical (**1**), a well-characterized molecular verdazyl-stacked structure including a ferrocene moiety as a spacer (see Figure 1), have evidenced a diamagnetic behavior up to room temperature.[27] The low-energy properties of this system are mainly governed by the unpaired electrons localized upon the verdazyl units. A lower limit of ∼2000 cm^{-1} for the absolute value of the exchange coupling constant $J = E(S = 0) - E(S = 1)$ has been suggested in this π-stacked structure. Several verdazyl-stacked structures have been reported in the literature,[7,12] forcing the $\pi-\pi$ interactions through the introduction of intermolecular or intramolecular constraints as in **1**.

Thus, we felt that the amplitude and origin of this antiferromagnetic exchange coupling constant should deserve particular attention. Indeed, so large an interaction is rather puzzling considering the relatively long distance (∼3.2 Å) between the spin carriers. Moreover, the closed-shell electronic structure of the ferrocene moiety may induce a through-space dialogue between the two verdazyl radicals. Using a multireference ab initio wave function, one can rigorously

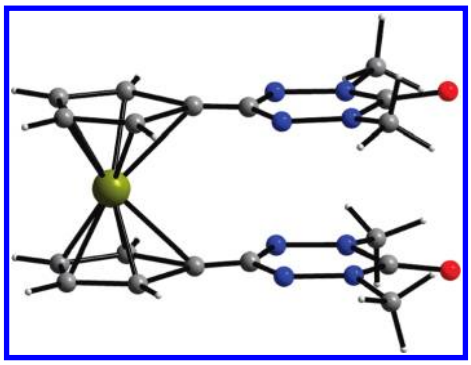

Figure 1. Synthetic compound **1** exhibiting a parallel face-to-face arrangement of two verdazyl radicals under the constraint of a ferrocene spacer.[27]

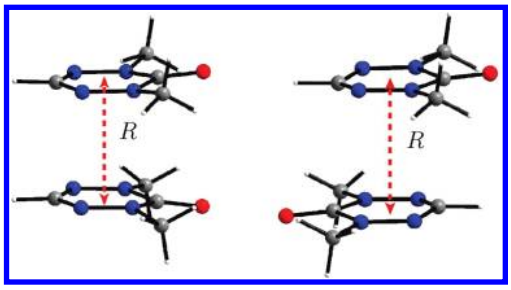

Figure 2. Archetypal units of verdazyl-based materials: C_s symmetry parallel face-to-face (left); C_i symmetry antiparallel face-to-face (right) verdazyl-based dimers.

extract the resonance integral t and Coulomb electron−electron repulsion energy U, which mostly determine the exchange coupling constant through the $4t^2/U$ ratio. Despite the system size, such calculations should thus complement the strategy which has been recently developed in selenazyl radical-based materials.[23] In addition, considering the J value in **1**, a reduction of the $4t^2/U$ ratio to lower values would be desirable to design new materials with improved magnetic properties. However, this criterion might be incompatible with the need for large t values to offset the Coulomb repulsion U, a prerequisite to produce itinerant electrons. Indeed, the resonance integral controls the bandwidth W, with $W = 4|t|$ for a 1D system. The evaluation of t and U parameters would bring some important insights into the properties of neutral radical-based compounds, as recently proposed for phenalenyl radical π dimers.[28]

In the present work, we use multireference wave-function-based calculations (difference dedicated configurations interaction method, DDCI[29]) to first evaluate the singlet−triplet energy difference J in complex **1**. The electronic role of the ferrocene spacer is analyzed by selecting the different exchange pathways. By removing the ferrocene moiety, the variations of J in systems consisting of two stacked-verdazyl radicals are reported as a function of the separation distance R (see Figure 2). Using coupled-cluster CCSD(T)- and density functional theory (DFT)-based calculations, the singlet and triplet state energies are evaluated with respect to R. Then, the relative spin-state ordering was examined with respect to temperature-induced lattice deformations, namely, the slippage of the π stacks[23,24] and their relative

(14) Kepenekian, M.; Le Guennic, B.; Awaga, K.; Robert, V. *Phys. Chem. Chem. Phys.* **2009**, *11*, 6066–6071.
(15) Norel, L.; Chamoreau, L.-M.; Journaux, Y.; Oms, O.; Chastanet, G.; Train, C. *Chem. Commun.* **2009**, 2381–2383.
(16) Norel, L.; Chamoreau, L.-M.; Train, C. *Polyhedron* **2009**, [online] DOI: 10.1016/j.poly.2009.05.065.
(17) Haddon, R. C. *Nature* **1975**, *256*, 394–396.
(18) Matsushita, M. M.; Kawamaki, H.; Sugawara, T.; Ogata, M. *Phys. Rev. B* **2008**, *77*, 195208.
(19) Camarero, J.; Coronado, E. *J. Mater. Chem.* **2009**, *19*, 1678–1684.
(20) Sugawara, T.; Matsushita, M. M. *J. Mater. Chem.* **2009**, *19*, 1738–1753.
(21) Ferrer, J.; Garcia-Suarez, V. M. *J. Mater. Chem.* **2009**, *19*, 1696–1717.
(22) Mandal, S. K.; Samanta, S.; Itkis, M. E.; Jensen, D. W.; Reed, R. W.; Oakley, R. T.; Tham, F. S.; Donnadieu, B.; Haddon, R. C. *J. Am. Chem. Soc.* **2006**, *128*, 1982–1994.
(23) Leitch, A. A.; Yu, X.; Winter, S. M.; Secco, R. A.; Dube, P. A.; Oakley, R. T. *J. Am. Chem. Soc.* **2009**, *131*, 7112–7125.
(24) Fujita, W.; Awaga, K. *Science* **1999**, *286*, 261–262.
(25) Brusso, J. L.; Clements, O. P.; Haddon, R. C.; Itkis, M. E.; Leitch, A. A.; Oakley, R. T.; Reed, R. W.; Richardson, J. F. *J. Am. Chem. Soc.* **2004**, *126*, 8256–8265.
(26) Beer, L.; Brusso, J. L.; Haddon, R. C.; Itkis, M. E.; Kleinke, H.; Leitch, A. A.; Oakley, R. T.; Reed, R. W.; Richardson, J. F.; Secco, R. A.; Yu, X. *J. Am. Chem. Soc.* **2005**, *127*, 18159–18170.
(27) Koivisto, B. D.; Ichimura, A. S.; McDonald, R.; Lemaire, M. T.; Thompson, L. K.; Hicks, R. G. *J. Am. Chem. Soc.* **2006**, *128*, 690–691.
(28) Huang, J.; Kertesz, M. *J. Phys. Chem. A* **2007**, *111*, 6304–6315.
(29) Miralles, J.; Castell, O.; Caballol, R.; Malrieu, J.-P. *Chem. Phys.* **1993**, *172*, 33–43.

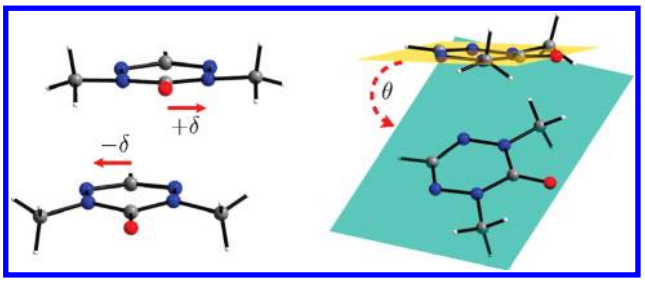

Figure 3. Slippage amplitude δ of the verdazyl radicals, one with respect to the other (left). Relative orientation of the verdazyl groups characterized by θ in a rotated face-to-face arrangement (right).

orientation (see Figure 3). Our goal is to investigate the possibility of spontaneous bond formation and to evidence by means of ab initio calculations a spin-transition-like behavior in this class of materials. Indeed, one important challenge is to rationally design bistable materials using microscopic observations,[30,31] and verdazyl radicals appear as remarkable candidates.

The relevant t and U parameters are simultaneously calculated with respect to R to (i) grasp the intermolecular interaction range in such archetypal organic-based material and (ii) clarify the origin of this intermediate regime featuring relatively large antiferromagnetic interactions which might afford metallic and self-assembling behaviors. Despite the system size and complexity, our calculations aim at defining on a rational footing organic-based systems with original properties such as spin-transition behavior.

2. Computational Details

It is known that some care must be taken to properly define the energy spectrum of open-shell systems.[32−35] However, spectroscopic accuracy can be reached using complete active space self-consistent field (CASSCF) and subsequent correlation effects treatments. Indeed, the CASSCF method gives reasonable electron distribution and accounts for the leading electronic configurations. Both the DDCI variational method[29] and second-order perturbation theory treatment (CASPT2) calculations have demonstrated their ability to rationalyze low-energy spectroscopies in various molecular and extended systems.[36−39] Thus, CASSCF calculations were first performed upon the reported crystal structure of **1**. The active space (CAS) includes the anticipated unpaired electrons and molecular orbitals (MOs) of the system, leading to a CAS[2,2] (i.e., two electrons in two MOs). Since the unpaired electron is likely to spin-polarize the inner shells,[10] a bare-valence picture limited to CAS[2,2]SCF calculations is undoubtedly unsatisfactory, and accuracy calls for demanding CI expansions. All our CASSCF and coupled-cluster CCSD(T) calculations were performed using the Molcas7.2 package.[40] All atoms were described using ANO RCC-type atomic functions.[40−42] Carbon, nitrogen, and oxygen atoms were described with (14s 9p 4d 3f 2g)/[3s 2p 1d] (i.e., DZP-type) contractions, whereas a (21s 15p 10d 6f 4g 2h)/[5s 4p 2d 1f] contraction was used for the iron atom. Finally, the hydrogen atoms were depicted using a minimal basis set contraction (8s 4p 3d 1f)/[1s].

Whatever the definition of the active space, it has been clearly demonstrated that the exchange interaction cannot be accurately evaluated ignoring the dynamical correlation phenomena.[43,44] For a given geometry, the dynamical polarization and correlation effects were then included using the DDCI method as implemented in the CASDI code.[45] As the number of degrees of freedom (i.e., holes in doubly occupied MOs, particles in virtual MOs of the CASSCF wave function) increases, one generates the successive DDCI-1, DDCI-2, and DDCI-3 CI spaces, as discussed in the literature for related compounds.[10] To eliminate the arbitrariness of the set of MOs in the DDCI calculations, natural orbitals were first generated by averaging the DDCI-1 density matrices of the singlet and triplet states. This procedure was iterated until convergence upon the energies was reached.[46] Using this iterated set of MOs, the singlet−triplet energy differences (i.e., J values) were then computed at the DDCI-3 level in the synthetic complex **1**, and in the stacked C_i and C_s verdazyl dimers as a function of the interplanar separation R (see Figure 2). A reading of the wave functions is very insightful into the mechanisms which govern the spin-state energy separation. The information extracted from the large CI calculations can be projected into the valence space using the effective Hamiltonian theory.[43,44] Considering the valence active space constructed on the singly occupied MOs (SOMOs) of the verdazyl radicals, the model space consists of a unique triplet and three singlet states. While the singlet−triplet DDCI-3 energy difference directly gives access to J, the two low-lying singlet wave functions can be projected onto the model space to simultaneously evaluate the resonance integral t, the Coulomb repulsion energy U, and the exchange interaction K ($J = 2K - 4t^2/U$).[43,44] The t and U integrals were estimated to investigate the origin of the large antiferromagnetic interaction in complex **1** and to evaluate the effective interaction range in prototype organic-based materials.

Complementary coupled-cluster CCSD(T) calculations were performed to evaluate the triplet state energy variations. Indeed, the monodeterminental character of the triplet state allows for a CCSD(T) energy, $E^{\mathrm{ref}}(S = 1)$, evaluation. From the accurate DDCI-3 J values, the singlet state potential energy curve was then reconstructed as $E(S = 0) = E^{\mathrm{ref}}(S = 1) + J$ to examine the possibility of bond formation in the diamagnetic state. The main characteristics of this distance-dependent behavior were examined for both spin states. In the vicinity of the equilibrium distances, the influence of the rotation angle θ of one verdazyl plane with respect to the other was investigated (see Figure 2). Along this deformation, the symmetry element is lost and disposes the CCSD(T) inspection due to size limitation.

(30) Kepenekian, M.; Le Guennic, B.; Robert, V. *Phys. Rev. B* **2009**, *79*, 094428.
(31) Kepenekian, M.; Le Guennic, B.; Robert, V. *J. Am. Chem. Soc.* **2009**, *131*, 11498–11502.
(32) Messaoudi, S.; Robert, V.; Guihéry, N.; Maynau, D. *Inorg. Chem.* **2006**, *45*, 3212–3216.
(33) Le Guennic, B.; Petit, S.; Chastanet, G.; Pilet, G.; Luneau, D.; Ben Amor, N.; Robert, V. *Inorg. Chem.* **2008**, *47*, 572–577.
(34) Le Guennic, B.; Robert, V. *C. R. Chim.* **2008**, *11*, 650–664.
(35) Herebian, D.; Wieghardt, K. E.; Neese, F. *J. Am. Chem. Soc.* **2003**, *125*, 10997–11005.
(36) Sadoc, A.; de Graaf, C.; Broer, R. *Phys. Rev. B* **2007**, *75*, 165116.
(37) Pierloot, K.; Vancoillie, S. *J. Chem. Phys.* **2006**, *125*, 124303.
(38) Kepenekian, M.; Robert, V.; Le Guennic, B.; de Graaf, C. *J. Comput. Chem.* **2009**, *30*, 2327–2333.
(39) Le Guennic, B.; Borshch, S.; Robert, V. *Inorg. Chem.* **2007**, *46*, 11106–11111.
(40) Karlström, G.; Lindh, R.; Malmqvist, P.-A.; Roos, B. O.; Ryde, U.; Veryazov, V.; Widmark, P.-O.; Cossi, M.; Schimmelpfennig, B.; Neogrady, P.; Seijo, L. *Comput. Mater. Sci.* **2003**, *28*, 222–239.
(41) Almlöf, J.; Taylor, P. R. *J. Chem. Phys.* **1990**, *92*, 551–560.
(42) Roos, B. O.; Lindh, R.; Malmqvist, P.-A.; Veryazov, V.; Widmark, P.-O. *J. Phys. Chem. A* **2005**, *109*, 6575–6579.
(43) Calzado, C. J.; Cabrero, J.; Malrieu, J. P.; Caballol, R. *J. Chem. Phys.* **2002**, *116*, 2728–2747.
(44) Calzado, C. J.; Cabrero, J.; Malrieu, J. P.; Caballol, R. *J. Chem. Phys.* **2002**, *116*, 3985–4000.
(45) Ben Amor, N.; Maynau, D. *Chem. Phys. Lett.* **1998**, *286*, 211–220.
(46) Garcia, V. M.; Castell, O.; Caballol, R.; Malrieu, J.-P. *Chem. Phys. Lett.* **1995**, *238*, 222–229.

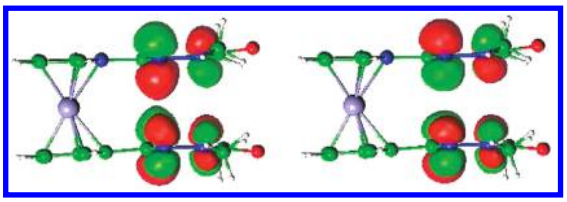

Figure 4. CAS[2,2] active orbitals for compound **1**.

Table 1. Calculated Magnetic Constant J (cm^{-1}) by Selecting Different Exchange Pathways (**1**, **1a**, and **1b**), at a DDCI-3 Level of Calculation

	1	**1a**	**1b**
J (cm^{-1})	−1340	−1270	−1370

Finally, a broken-symmetry approach[47] allowed us to assess the reliability of DFT calculations in the determination of low-energy properties of this class of materials. Indeed, the system size would naturally call for such methodology. The DFT calculations were performed using the 2008.01 version of the ADF program[48,49] with both the pure GGA (generalized gradient approximation) BP86 functional of Becke and Perdew[50−52] and the three-parameter hybrid functional of Becke based on the correlation functional of Lee, Yang, and Parr (B3LYP).[53,54] All atoms were described with triple-ζ (TZP) basis sets.

3. Results

3.1. Magnetic Properties of Compound 1. Starting from the reported crystal structure of **1**, CAS[2,2] calculations were first performed, and dynamical correlation contributions were then included variationally (DDCI-3 level) to evaluate the singlet−triplet gap. As expected, the magnetic orbitals correspond to the in-phase and out-of-phase linear combinations of the singly occupied verdazyl molecular orbitals (SOMOs in Figure 4). Following the iterative DDCI philosophy, the singlet−triplet energy difference J was estimated at the DDCI-3 level. These results are summarized in Table 1. Interestingly, the resulting exchange coupling constant J is calculated to be -1340 cm^{-1}, a value which is consistent with the experimental temperature-dependent magnetic susceptibility measurements reflecting a diamagnetic behavior. Even though the radical separation is rather large, this value is suggestive of a strong antiferromagnetic regime, the origin of which should be unraveled.

In order to quantify the different magnetic exchange pathways, similar DDCI-3 calculations were performed by (i) freezing the MOs localized on the ferrocene moiety and (ii) replacing the iron center by a +2 point charge. The former strategy referred to as **1a** enlightens the direct "through-space" magnetic interactions between the radicals, whereas the latter, **1b**, stresses the role of the iron center as a magnetic coupler (see Figure 5). Along this analysis, the traditional picture of magnetic systems is reconsidered. Indeed, the respective roles of the ligand and spin carriers are inverted in **1**. From the comparison of the J values given in Table 1, one can conclude that the exchange constant is greatly dominated by the direct through-space exchange pathway between the nitrogen-rich parts of the verdazyl radicals (**1** versus **1a**). Starting from **1a**, the substituents upon the verdazyl radicals (i.e., cyclopentadienyl) bring an additional 100 cm^{-1} antiferromagnetic contribution, to perfectly recover the J value in **1** (**1** versus **1b**). As a main conclusion of this inspection, the Fe^{2+} ion turns out to be innocent in the exchange coupling mechanism, which is essentially developed on the verdazyl parts.

3.2. Magnetic Properties of Stacked Verdazyls. Since the magnetic properties can be totally ascribed to the verdazyl radicals, we then concentrated on purely organic packings (see Figure 2). Our goal was two-fold. First, we were concerned with the modulation of the magnetic interaction in such an arrangement to evaluate the distance-dependent hopping and one-site repulsion energy parameters. Then, considering the strong antiferromagnetic behavior, one may wonder whether a bound species can be predicted from the interaction of two verdazyl-based radicals.

In order to provide a detailed analysis of the electronic properties and hence a guide for future experimental works, we performed a series of calculations on stacked verdazyl radicals. Different packing architectures, as exemplified in Figure 2, have been reported in the literature.[7,12] Therefore, diradical parallel and antiparallel face-to-face systems were considered (see Figure 2). The J values at a DDCI-3 level of calculations are shown in Figure 6 as a function of the interplanar separation R. First, whatever the distance, the systems are antiferromagnetic. However, the exchange coupling constant $|J|$ is reduced in the antiparallel arrangement as opposed to the parallel one (see Figure 6). Such behavior is a reflection of the nonstrictly equivalent character of the nitrogen atoms due to the presence of the electron-withdrawing oxygen atom. The overlap between the verdazyl SOMOs is greatly modified from one arrangement to the other. With a magnetic material preparation goal in mind, this result suggests that antiparallel face-to-face organization should be favored to avoid a diamagnetic regime.

Using the J values, the effective parameters governing the singlet−triplet splitting were then extracted from the multireference DDCI-3 wave functions. Such a procedure uses the effective Hamiltonian theory as previously reported.[43,44] Since the verdazyl−verdazyl distance is rather large and strong antiferromagnetism prevails, the effective exchange contribution K is expected to be negligible and J reduces to $-4t^2/U$. Indeed, whatever the arrangement, $|K|$ is ∼20 cm^{-1} from our calculations. The resonance integral and Coulomb repulsion energy were evaluated in both dimers as a function of R. In the vicinity of the typical inter-radical distance of ∼3.2 Å reported in the literature, U is not greatly modified (see Figure 7). Relative changes smaller than 8% are observed for important radical−radical distance modifications up to 10%. For comparison purposes, Table 2 summarizes the Coulomb repulsion energies extracted from DDCI-3 calculations in the ethylene molecule considered as a

(47) Noodleman, L.; Case, D. A. *Adv. Inorg. Chem.* **1992**, *38*, 423–470.
(48) *ADF2006.01*, SCM; Theoretical Chemistry, Vrije Universiteit, Amsterdam, The Netherlands, 2006.
(49) te Velde, G.; Bickelhaupt, F. M.; Baerends, E. J.; van Gisbergen, S. J. A.; Fonseca Guerra, C.; Snijders, J. G.; Ziegler, T. *J. Comput. Chem.* **2001**, *22*, 931–967.
(50) Becke, A. D. *Phys. Rev. A* **1988**, *38*, 3098–3100.
(51) Perdew, J. P. *Phys. Rev. B* **1986**, *33*, 8822–8824.
(52) Perdew, J. P. *Phys. Rev. B* **1986**, *34*, 7406–7406.
(53) Lee, C.; Yang, W.; Parr, R. G. *Phys. Rev. B* **1988**, *37*, 785–789.
(54) Becke, A. D. *J. Chem. Phys.* **1993**, *98*, 5648–5852.

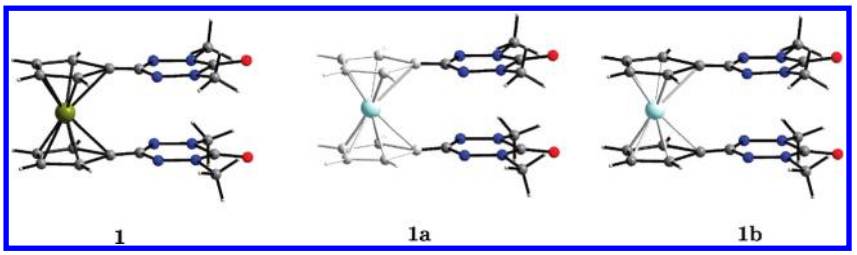

Figure 5. Different approximations of the magnetic interactions by selectively turning on specific pathways. The shaded parts indicate the pathways which are turned off in the calculations for analysis purposes.

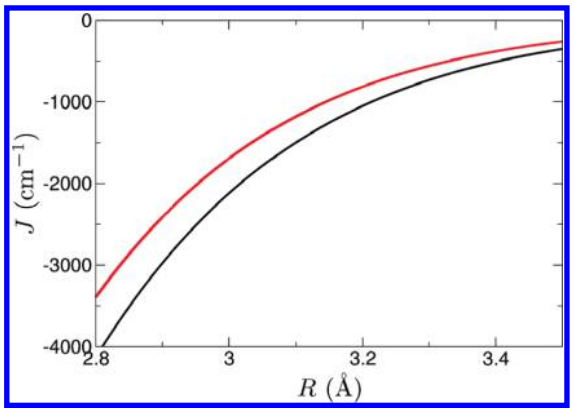

Figure 6. Variations of the magnetic constants J (cm^{-1}) as a function of R (Å) for the parallel face-to-face packing (black curve) and antiparallel face-to-face packing (red curve).

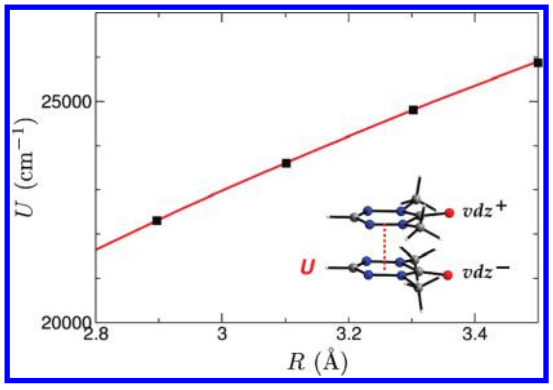

Figure 7. Variation of the Coulomb repulsion U (cm^{-1}) in the parallel face-to-face dimer as a function of R (Å).

Table 2. Coulomb Repulsion Values U (cm^{-1}) Extracted from the DDCI-3 Singlet−Triplet Energy Difference

	ethylene	$[Cu_2(\text{-}\mu CH_3COO)_4(H_2O_2)]$	**1**
U (cm^{-1})	59780	60410	23858

hypothetical magnetic system, and the archetypal magnetic system $[Cu_2(\mu CH_3COO)_4(H_2O_2)]$.[55] In such systems, the U values can be attributed either to mainly 2p-type or diffuse 3d-type atomic orbitals. From our ab initio inspection, the intrinsically delocalized character of the magnetic orbitals in **1** significantly reduces (by a factor of ~3) the Coulomb repulsion. Indeed, U reflects the ability of a verdazyl ligand to accommodate one additional electron. Thus, it determines the amplitude

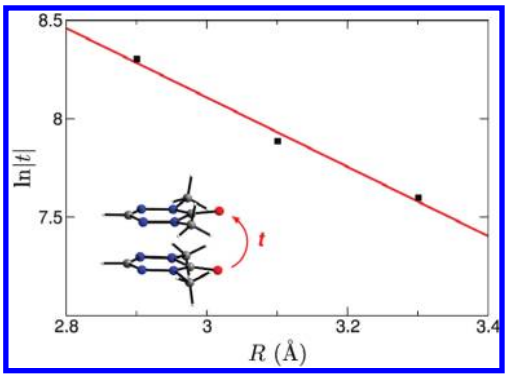

Figure 8. Log plot of the effective resonance parameter t as a function of R (Å) for the parallel face-to-face arrangement. Similar behavior is observed for the antiparallel one.

of the charge disproportionation mechanism $vdz^{\bullet} - vdz^{\bullet} \rightarrow vdz^{+} - vdz^{-}$, featuring the electron delocalization in the solid state. As seen in Figure 7, the larger the distance separation, the larger the Coulomb repulsion. The Coulomb stabilization energy arising in the $vdz^{+} - vdz^{-}$ electronic configuration is reduced as the two radicals are pulled apart. Thus, the radical units should be brought as close as possible to enhance the conduction properties, a scenario which simultaneously favors the SOMO overlap and a wider bandwidth W.

As expected, the resonance parameter t is very sensitive to the interplanar verdazyl−verdazyl distance. The exponential decay of t (see Figure 8) is a measure of the interaction range which controls the solid state bandwidth. We found that these values (0.57 Å) are very similar in both arrangements. This is a clear indication that, beyond ~4 Å, the exchange interaction vanishes along with the transport properties. Thus, the introduction of a chemical spacer such as ferrocene in compound **1** looks like a very promising synthetic strategy since the radical−radical distance is controlled below this critical distance value. Nevertheless, a larger distance would be desirable to effectively reach a magnetic regime where the singlet and triplet states compete at room temperature.

Finally, the singlet and triplet states' total energy of the parallel and antiparallel face-to-face dimers were examined as a function of the distance separation (see Figure 9). Despite the widespread popularity and success of DFT, it is known that its applications suffer from qualitative failures such as the energies of dissociating molecular systems. As stated in the literature, this methodology "has been the most useful for systems of very many electrons".[56]

(55) Guha, B. *Proc. R. Soc. London* **1951**, *206*, 353–373.

(56) Kohn, W. *Rev. Mod. Phys.* **1999**, *71*, 1253–1266.

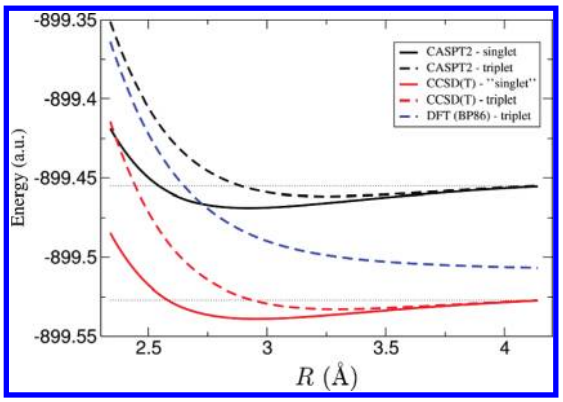

Figure 9. Singlet and triplet total energies (atomic units, au) in the parallel face-to-face arrangement as a function of R (Å). The curves have been shifted for clarity. The DFT broken symmetry curve is totally superimposable to the triplet one and has not been represented.

Nevertheless, the reliability of such a method for weak bond formation and open-shell system issues is questionable. Discarding the "exponential wall",[56] we also examined whether specific wave-function-based calculations can afford for a rigorous treatment of this emerging class of organic systems to be conducted. Starting from the monodeterminantal triplet reference CCSD(T) energies $E^{ref}(S = 1)$, the DDCI-3 J value was added to evaluate the singlet energy at each interplanar distance R, as $E(S = 0) = E^{ref}(S = 1) + J$. As a matter of fact, the singlet-state wave function exhibits a non-negligible multireference character which disposes a straight CCSD(T) treatment.

Let us first concentrate on the triplet potential energy curve which was compared to DFT calculations (see Figure 9). The explicitly correlated calculations (CCSD(T)) exhibit a shallow minimum for $R_{eq}(S = 1) = 3.34$ Å with a binding energy of 27 kJ mol^{-1}. In contrast, the DFT curve is dissociative, whatever the exchange functional used (B3LYP or BP86). Despite the acceptable single reference approximation for the triplet state, the absence of dispersion interactions along the DFT framework might be responsible for this behavior.

Using a broken-symmetry approach,[47] the singlet energy was also calculated and a dissociative character observed. This failure due to the use of an approximate exchange-correlation functional is rather puzzling since the DFT binding energy of the simplest analogue H_2 is severely overestimated.[57] This is to be contrasted with the wave-function-based potential of the $S = 0$ state, which is suggestive of a bound system. Indeed, as the spin state changes from $S = 1$ to $S = 0$, the minimum position is down-shifted by 0.4 Å ($R_{eq}(S = 0) = 2.94$ Å) with a binding energy of 43 kJ mol^{-1} (see Figure 9). The antiferromagnetic behavior can be seen as a self-assembly ability in verdazyl stacks, a rather remarkable characteristic for this class of organic materials. To validate this puzzling observation, complementary CASPT2 (complete active space self-consistent field and subsequent second-order perturbation treatment) calculations were performed for both spin states (see Figure 9). The active space was enlarged to CAS[18,14], including all of the verdazyl π electrons and MOs. A similar trend is observed for both arrangements with a shortening of the verdazyl−verdazyl distance along the $S = 1$ to $S = 0$ transition. This is one important theoretical observation on which we would like to comment. A standard way to fit temperature-dependent magnetic susceptibility measurements is to introduce a magnetic exchange coupling constant, J, which is assumed to be constant in the temperature range. The underlying assumption in such procedure is that the crystal structure is not greatly affected by the temperature modifications. In light of our theoretical investigation, such a hypothesis is more than questionable since a non-negligible lattice expansion might be anticipated along the singlet-to-triplet change. Ideally, temperature-dependent X-ray data should complement the magnetic susceptibility measurements. Similar conclusions were drawn recently since it has been experimentally demonstrated that the exchange interaction can be changed by an order of magnitude.[58]

4. Discussion

The magneto-structural correlations which have emerged from our calculations are also suggestive of a possible spin-crossover behavior. Indeed, our results suggest that stacked verdazyl dimers are likely to spontaneously form bound singlet and triplet species. The expected, and here quantified, interplanar distance expansion supports the possibility to induce such a phenomenon. While examples of polymorphism in neutral organic radicals are still scarce,[59−62] hysteretic behavior has been observed in such radical materials.[24,25,63] However, very few structural changes have been observed (∼3%) in these dithiazolyl radicals when the temperature was modified. In the present study, the simultaneous existence of bound spin states, a prerequisite to observing such a phenomenon, could be at the origin of similar bistable organic radical-based compounds. Clearly, the weak bond regime which is achieved in this class of materials might be at the origin of simultaneous temperature-induced spin and bond distance changes. One may expect a reduction of the $|J|$ value upon heating (see Figure 10). In addition, a significant softening of the corresponding vibrational mode is calculated since the curvature of the $S = 1$ curve is twice as small as the $S = 0$ one. It is known that this phenomenon enhances the driving entropic contributions. Clearly, other structural changes, not to mention the existence of interdimer interactions in the synthetic materials, should also be included.

Nevertheless, the singlet remains in the ground state over the whole interplanar distance range, as summarized in Figure 10. Such behavior disposes of the possibility to observe spin-transition. Some specific chemical modifications might however change this state of affairs.

(57) Baerends, E. J. *Phys. Rev. Lett.* **2001**, *87*, 133004.

(58) Veber, S. L.; Fedin, M. V.; Potapov, A. I.; Maryunina, K. Y.; Romanenko, G. V.; Sagdeev, R. Z.; Ovcharenko, V. I.; Goldfarb, D.; Bagryanskaya, E. G. *J. Am. Chem. Soc.* **2008**, *130*, 2444–2445.

(59) Bond, A. D.; Haynes, D. A.; Pask, C. M.; Rawson, J. M. *J. Chem. Soc., Dalton Trans.* **2002**, 2522–2531.

(60) Clarke, C. S.; Pascu, S. I.; Rawson, J. M. *CrystEngComm* **2004**, *6*, 79–82.

(61) Leitch, A. A.; McKenzie, C. E.; Oakley, R. T.; Reed, R. W.; Richardson, J. F.; Sawyer, L. D. *Chem. Commun.* **2006**, 1088–1090.

(62) Alberola, A.; Clements, O. P.; Collis, R. J.; Cubbitt, L.; Grant, C. M.; Less, R. J.; Oakley, R. T.; Rawson, J. M.; Reed, R. W.; Robertson, C. M. *Cryst. Growth Des.* **2008**, *8*, 155–161.

(63) Barclay, T. M.; Cordes, A. W.; George, N. A.; Haddon, R. C.; Itkis, M. E.; Mashuta, M. S.; Oakley, R. T.; Patenaude, G. W.; Reed, R. W.; Richardson, J. F.; Zhang, H. *J. Am. Chem. Soc.* **1998**, *120*, 352–360.

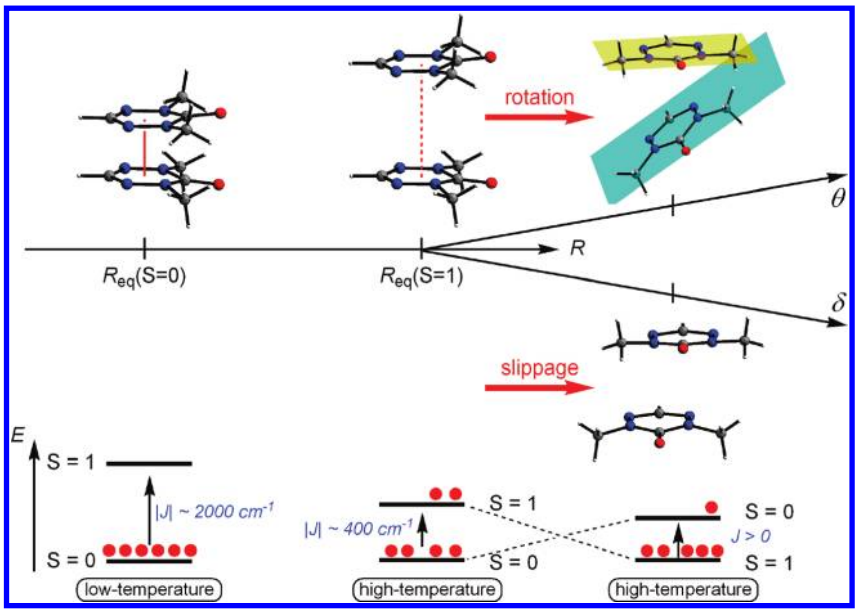

Figure 10. Schematic representation of the singlet−triplet splitting as the interplanar distance R is changed from the calculated singlet to triplet equilibrium distance. The slippage δ and relative orientation θ of the verdazyl rings eventually stabilize the triplet over the singlet, featuring a spin-transition phenomenon. The red beads stand for the dimer stacks in the hypothetical materials.

Table 3. DDCI-3 J Values (cm^{-1}) with Respect to the Slippage Amplitude δ (Å) at the Calculated Equilibrium Distance R_{eq} (S = 1) = 3.34 Å of the Triplet State

δ	0.3	0.4	0.5	0.6	0.7	0.8
J	−365	−217	−86	+5	+47	+45

Table 4. DDCI-3 J Values (cm^{-1}) with Respect to the Relative Orientation of the Verdazyl Rings (θ, deg) at Different Verdazyl−Verdazyl Distances (R, Å)

	θ				
R	30	35	**40**	**45**	50
3.30	−732	−535	**−208**	**+185**	+379
3.35	−593	−632	**−155**	**+166**	+326
3.40	−464	−335	**−107**	**+156**	+253
3.45	388	−262	**−68**	**+150**	+216

In light of the experimental data available for thiazyl radicals[24] and recent theoretical inspections,[23] we looked into the slippage (see Figure 3) influence on the singlet−triplet energy difference. The geometry change is not compatible with the initial structure of compound **1** and would require supplementary experimental works. However, this mechanism was evidenced as the temperature is modified and is expected to reduce the SOMO overlap. Therefore, such distortion should favor a ferromagnetic interaction since the hopping integral is reduced. The influence of δ at the S = 0 and S = 1 equilibrium distances was examined using DDDI-3 calculations. As seen in Table 3, the ground state becomes triplet for $\delta \sim 0.6$ Å, a value which is consistent with the slippage value (~1.32 Å) experimentaly reported in the 1,3,5-trithia-2,4,6-triazapentalenyl analog.[24]

Then, we thought that a promising strategy would be to modify the relative orientation of the verdazyl rings (see Figure 2), a mechanism which is likely to reduce the hopping integral. Since the rotation may be accompanied by an interplanar distance change, the singlet−triplet energy differences were calculated in the vicinity of the triplet verdazyl−verdazyl equilibrium distance. As expected, $|J|$ is reduced as

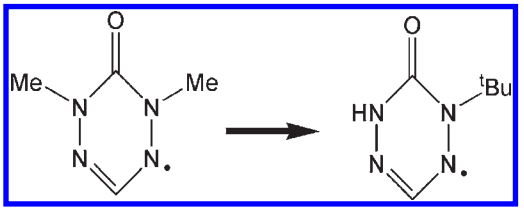

Figure 11. Proposed ligand substitution to force the relative orientation of the verdazyl rings.

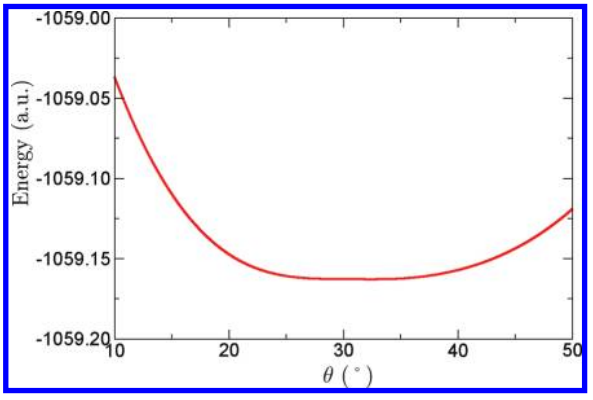

Figure 12. DFT triplet state energy (au) as a function of the relative orientation θ (deg) of the verdazyl rings.

θ increases, and eventually the triplet state becomes the ground state for $\theta \sim 42°$ (see Table 4).

Inspection of the potential energy surface difference shows that the critical θ value is almost unsensitive to the interplanar distance in the 3.30−3.45 Å range (see Table 4). We checked that the initial antiferromagnetic picture ($J < 0$) is not affected in the small distance regime. Quantitatively, for R = 2.95 Å and $\theta = 45°$, the J value is -636 cm^{-1}. Thus, one may expect to establish a spin transition behavior in such compounds by forcing the relative orientation of the verdazyl rings.

To support this strategy, we finally introduced bulky terbutyl groups and hydrogen atoms in the constitutive verdazyl radical unit (see Figure 11). These substitutions are likely to afford a relative orientation as a consequence of the steric hindrance. Complementary DFT optimizations were performed for the triplet state to evaluate the impact of such chemical changes. Clearly, a full geometry optimization would not be conclusive since we have shown that DFT fails to produce a bound state. In contrast, a constrained geometry optimization where all coordinates but the angle between both verdazyl moieties are kept frozen may bring some qualitative information (see Figure 12). The steric hindrance resulting from the presence of bulky ligands forces the relative rotation of the verdazyl radicals. Interestingly, a relative orientation of ~35° between the verdazyl rings is found, a value which supports the proposed strategy.

5. Conclusion

In conclusion, the exchange interactions were analyzed in synthetic and hypothetical verdazyl-based compounds using multireference calculations. The simultaneous evaluation of the resonance integral t and Coulomb repulsion energy U from rigorous calculations brings some useful information regarding the different mechanisms. As a major observation, the reduction of the Coulomb repulsion accounts for the strong antiferromagnetic behavior. This phenomenon emerges from the delocalized character of the magnetic orbitals upon the nitrogen-rich part of the verdazyl radicals. From demanding CCSD(T) calculations and DDCI-3 exchange values, a shallow covalent bond well was observed for both singlet and triplet states, whereas the DFT approach fails to predict triplet and singlet bound states. In light of our inspection, verdazyl-based materials appear as remarkable candidates since the dimerization process through σ-bond-type formation is sufficiently smooth to simultaneously structure the material and give rise to magnetic properties. Finally, the 0.4 Å increase (10%) of the verdazyl−verdazyl equilibrium distance along with a relative rotation of the verdazyl rings is strongly suggestive of a possible $S = 0$ to $S = 1$ spin-crossover phenomenon, which calls for further experimental study. The slippage and relative orientation of the verdazyl radical rotation are expected to favor such an original scenario in verdazyl-stacked assemblies. Our work should provide the basis for future experiments in the preparation of original materials.

Acknowledgment. This work was developed within the "fdp magnets" project (ANR-07-JCJC-0045-0). The authors are thankful to C. Train and G. Pilet for helpful discussions, the reviewers for their useful suggestions, and to the "Institut de Développement et de Ressources en Informatique" (IDRIS) for computing facilities.